

Available online at [www.sciencedirect.com](http://www.sciencedirect.com)**ScienceDirect**

Procedia Structural Integrity 2 (2016) 597–603

Structural Integrity

**Procedia**[www.elsevier.com/locate/procedia](http://www.elsevier.com/locate/procedia)

21st European Conference on Fracture, ECF21, 20-24 June 2016, Catania, Italy

## Mechanical properties degradation of (Al-Cu-Li) 2198 alloy due to corrosion exposure

Nikolaos D. Alexopoulos<sup>a,\*</sup>, Angeliki Proiou<sup>a</sup>, Wolfgang Dietzel<sup>b</sup>, Carsten Blawert<sup>b</sup>,  
Volker Heitmann<sup>b</sup>, Mikhail Zheludkevich<sup>b</sup>, Stavros K. Kourkoulis<sup>c</sup>

<sup>a</sup>Department of Financial Engineering, University of the Aegean, 82 132 Chios, Greece

<sup>b</sup>Institute of Materials Research, Department of Corrosion and Surface Technology, Helmholtz-Zentrum Geesthacht, 21502 Geesthacht, Germany

<sup>c</sup>Lab of Testing and Materials, Dept of Mechanics, National Technical University of Athens, 9 Heroon Polytechniou Str., 15773 Athens, Greece

### Abstract

The present work investigates the corrosion resistance of the innovative Al-Cu-Li (2198) aluminum alloy; a comparison against Al-Cu (2024) alloy is attempted. Tensile specimens were pre-corroded for different exposure times to exfoliation corrosion solution and immediately afterwards they were tested in tension. For small exposure times (< 12 h) small pits could be found on the corroded surfaces; pitting was also noticed at the small side surfaces (thickness) of the tensile specimens. Corrosion exposure seems not to essentially decrease the yield stress of AA2198 even for high exposure times, while this was not the case for AA2024. After heavy corrosion exposure (>12 h), AA2024 lost almost 30% of its initial ultimate tensile strength, while for AA2198 the respective value was only 11%. Al-Cu-Li alloy shows superior corrosion resistance in terms of maintaining higher percentages of tensile ductility; AA2198 exhibited higher remaining elongation at fracture values due to corrosion degradation for all investigated exposure times.

Copyright © 2016 The Authors. Published by Elsevier B.V. This is an open access article under the CC BY-NC-ND license (<http://creativecommons.org/licenses/by-nc-nd/4.0/>).

Peer-review under responsibility of the Scientific Committee of ECF21.

**Keywords:** alloy 2024; alloy 2198; tension; artificial ageing; exfoliation corrosion; ductility

\* Corresponding author. Tel.: +0030-22710-35464; fax: +0030-22710-35429.

E-mail address: [nalexop@aegean.gr](mailto:nalexop@aegean.gr)

## 1. Introduction

The main driving force in aircraft structural design and aerospace material development is to reduce weight. Due to their high stiffness-to-weight and strength-to-weight ratios, aluminum alloys have been the dominant aircraft materials for many decades. In order to compete the decreasing tendency of Al usage in aero structures (in contrary to composite materials), aluminum alloy producers are making a huge effort in developing lighter and better weldable alloys. Li is added to Al-Cu alloys from the series 2xxx in a lower proportion than the Cu addition. They offer lower density than conventional aluminum alloys and direct weight reduction of about 5 %. The improved property balance i.e. corrosion resistance, fatigue crack growth rate, strength and toughness, allows further weight reduction up to 20% through adapted design, and reduction of aircraft maintenance costs. In order for the Al-Cu-Li alloy to replace the conventional one in aircraft structures, it has to be definitely proven that its mechanical behaviour, damage tolerance capabilities and corrosion resistance are at least equal or superior to its predecessor. Nevertheless, the literature about the mechanical behavior of the advanced Al-Cu-Li alloy seems to be rather limited. For example, Chen et al. (2011) performed tests on two different heat treated AA2198 (namely T351 and T851) and investigated their plastic and fracture behavior. Steglich et al. (2010a) and (2010b) investigated experimentally and analytically the anisotropic deformation of AA2198-T8 occurring during mechanical loading with and without the presence of artificial notches. Alexopoulos et al. (2013) have studied the fatigue mechanical properties of the advanced alloy and confirmed its superiority against its predecessor AA2024 in high-cycle fatigue and endurance limit regimes, especially when considering the specific mechanical properties of these alloys. Investigations on the corrosion resistance of AA2198 are even more limited.

In this direction an attempt is described in the present work to report experimental evidence regarding the corrosion potential of this alloy and directly compare the results against the respective one for the well-established AA2024. This work will focus on the comparison of the two alloys along with their resistance to corrosion, in terms of maintaining their tensile mechanical properties when pre-corroded for different exposure times.

## 2. Materials and experimental procedure

The materials used for the present investigation were AA2198 and AA2024 wrought aluminum alloys that were received in sheet form with nominal thicknesses of 3.2 mm. The weight percentage chemical composition of the 2198 alloy is <0.08 % Si, <0.01 % Fe, 2.9-3.5 % Cu, <0.5 % Mn, 0.25-0.8 % Mg, 0.8-1.1 % Li, 0.35 % Zn, 0.04-0.18 % Zr, 0.1-0.5 % Ag. Tensile specimens were machined along the longitudinal (L) direction of the material according to the ASTM E8 specification. Prior to corrosive solution exposure, all surfaces of the specimens were cleaned with alcohol according to ASTM G1 specification.

Table 1 shows the exposure corrosion times and the number of tensile specimens used in the present experimental protocol. Tensile specimens were exposed for different hours to the laboratory exfoliation corrosion environment (hereafter called EXCO solution) according to the ASTM G34 specification. The corrosive solution consisted of the following chemicals diluted in 1 l distilled water; sodium chloride (4.0M NaCl), potassium nitrate (0.5 KNO<sub>3</sub>) and nitric acid (0.1 M HNO<sub>3</sub>). Further details can be found in the respective specification. After the corrosion exposure the corroded specimens were immediately cleaned according to ASTM G34 and then they were subjected to tensile testing.

Table 1. Investigated exfoliation corrosion exposure times and number of tensile specimens.

	Different exposure times to EXCO solution										Total
	0 h	0.5 h	1 h	2 h	4 h	6 h	8 h	12 h	24 h	48 h	
# of spec. AA2024-T3	5	3	3	3	3	-	3	3	3	-	26
# of spec. AA2198-T3	5	-	-	3	-	3	-	3	3	3	20

Tensile tests were carried out using an INSTRON 100 kN servo-hydraulic testing machine. The tests were implemented according to the ASTM E8 specification. An external extensometer was properly attached at the reduced cross-section at the mid-height of the specimens' gauge length. Three specimens were tested in each different case to get reliable average data. A data logger was used during all the experiments and the values of load, displacement and axial strain were recorded and stored in a computer.

### 3. Results and discussion

One of the main goals of the present article is to investigate and compare the tensile mechanical behaviour of AA2024 and AA2198 after being exposed to corrosive solution. Tensile specimens of both alloys were exposed for different times to exfoliation (EXCO) solution. It is well known that for higher exposure times to corrosion solution, corrosion induced surface pits are formed that act as surface notches; they have profound effect on the ductility degradation of the specimen as they act as stress raisers.

Different corrosion exposure times were selected to corrode the reference material (without any ageing at the T3 condition) and their effect on the typical tensile flow curves can be seen in Figs. 1a and 1b for AA2024 and AA2198, respectively. The tensile test results for AA2024 were in detail reported by Alexopoulos et al. (2016), where after 2 h exposure a sudden drop on the tensile flow curve was noticed, Fig. 1a. This strength drop was associated with the effective thickness decrease of the specimens as a sequence of transverse cracks originated from corrosion-induced surface pits. Nevertheless, the decrease in tensile ductility couldn't be explained for the very low exposure times where no surface deterioration exists and therefore this ductility decrease was attributed to the hydrogen embrittlement effect. Likewise, the elongation at fracture seems to continuously decrease with increasing EXCO time exposure for AA2198, Fig. 1b. Nevertheless, no sudden drop in strength of the flow curves is noticed for the case of AA2198 that would be evidence for transverse pit-to-cracking defects and decrease of the effective cross-section of the specimens.

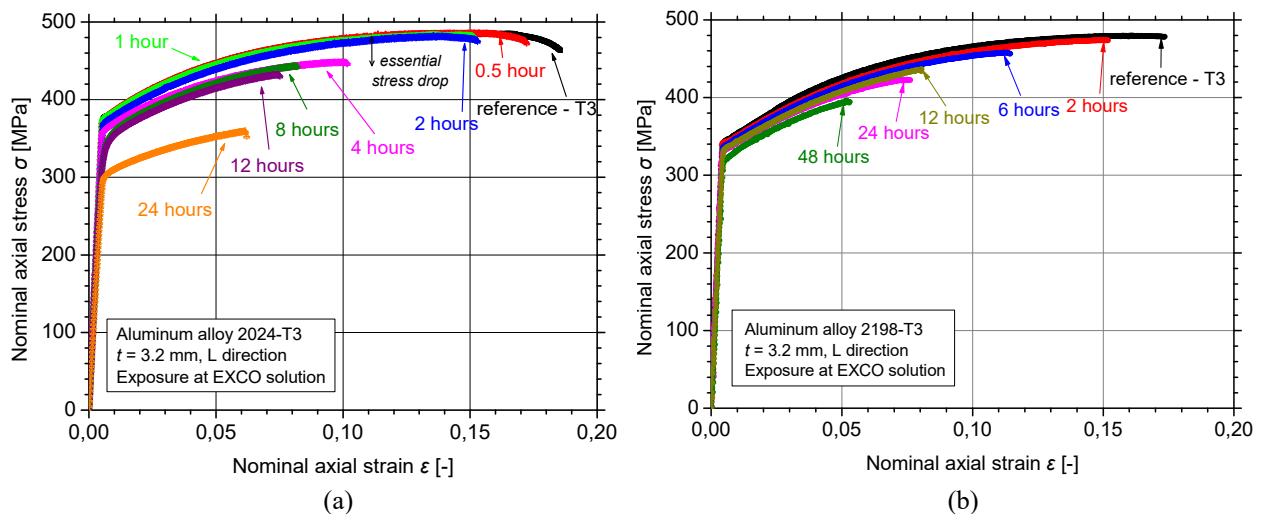


Fig. 1. Typical experimental tensile flow curves of corroded aluminum alloys (a) 2024; (b) 2198 specimens for different exposure times to exfoliation corrosion solution.

Typical specimens' surfaces of AA2198 when exposed for various corrosion exposure times can be seen in Fig. 2. Figs. 2a to 2c show the corroded surface when exposed for 2 h, 24 h and 48 h, respectively while Figs. 2d to 2f show the same surfaces of the specimens after the tensile test and fracture. It is evident from Fig. 2a that for the low exposure time (2 h) pitting in the corroded area of the tensile specimen is quite limited. In addition, the fracture path (shown in Fig. 2d) is almost perfectly normal to the direction of the axial load applied. Hence it seems that the fracture mechanism is not seriously influenced by the corrosion exposure.

More pitting is evident in the corroded surface of the 24 h exposed specimen in Fig. 2b. Unlike the previous

specimen, Fig. 2e shows that the fracture path of this specimen follows the weakest ligaments in the specimen surface. Evident is also the cracking density at the surface due to the tensile stretching; this implies the evidence of sub-surface damage of the specimen before tension.

Finally Fig. 2c shows excessive surface deterioration due to corrosion exposure. Small scale pitting as well as signs of excessive exfoliation is evident for the 48 hours exposure. Surface microcracking that was formed due to the application of axial loading can also be seen for this exposure time (Fig. 2f). In the sections following, each tensile mechanical property will be analyzed separately.

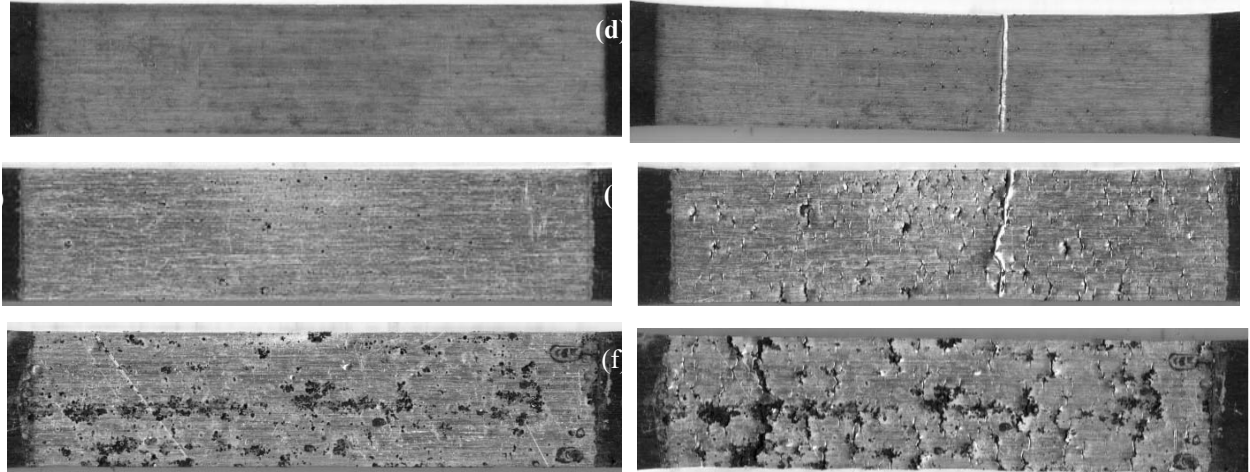


Fig. 2. Typical corroded surfaces of the tensile specimens of AA2198 for different exposure time: (a) 2 h; (b) 24 h; (c) 48 h; and (d) to (e) respective surfaces after tensile tests.

### 3.1. Effect on mechanical properties

#### 3.1.1. Conventional yield stress

Conventional yield stress  $R_{p0.2\%}$  was calculated based on the nominal cross-section of the specimen and without taking into account the effective thickness of the specimens. Fig. 3 shows the test results of AA2024 and AA2198 as average values and respective standard deviation derived from three specimens each. The available experimental test results were simply interpolated with the aid of a B-Spline curve (eye-catch) in order to roughly assess the corrosion

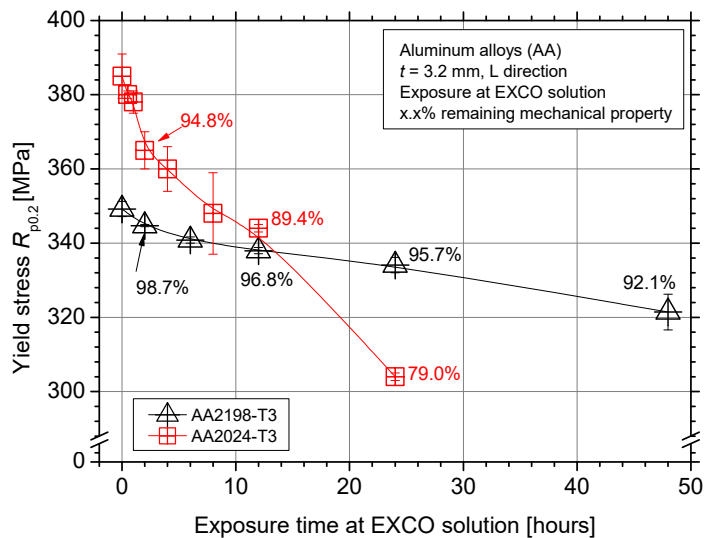


Fig. 3. The dependence of the yield stress on the exposure times at EXCO solution for the aluminum alloys 2024 and 2198.

exposure effect on the mechanical properties of the two aluminium alloys tested. AA2024 is significantly affected by corrosion exposure and its yield stress, shown in red squares, is essentially decreased; only 79% of the property remains after 24 hours exposure to the corrosive solution. On the contrary, this was not the case for AA2198, where the yield stress remains almost constant after heavily exposure to corrosion exposure (black triangles in Fig. 3) e.g. after 48 hours. A very small decrease is observed which could be perhaps attributed to the decrease of the effective thickness of the specimen.

### 3.1.2. Tensile strength

The values of the tensile strength  $R_m$  were again calculated by taking into account the nominal cross-sections of the specimens and the results are summarized in Fig. 4 (adopting the same notation and interpolation approach as in Fig. 3). Comparative consideration of the plots of Fig. 4 for the two aluminum alloys shows clearly that AA2024 degrades at significantly higher rates in comparison to AA2198 (for the same exposure time). It is mentioned characteristically that at 12 hours exposure almost 87% of the initial property remains for AA2024, while for AA2198 the respective value exceeds 92% of its initial value. Degradation decrease is essentially higher for 24 hours exposure, where the respective properties are equal to about 73% and 88% for the two alloys, respectively.

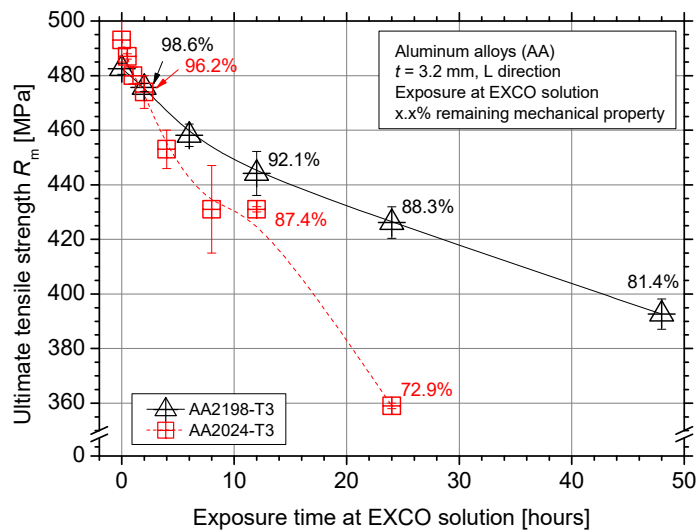


Fig. 4. The dependence of the tensile strength on the exposure times at EXCO solution for the aluminum alloys 2024 and 2198.

### 3.1.3. Elongation at fracture

The values of the elongation at fracture  $A_f$  of the pre-corroded tensile specimens can be seen in Fig. 5 (the same notation and interpolation approach as in Fig. 3 is followed) for both aluminum alloys studied in the present protocol. It can be seen from this figure that for relatively small exposure times (i.e. up to 6 hours) AA2024 degrades in higher rates than AA2198. This is really dangerous, since for low exposure times, no visual - surface signs (pits, etc) of the induced corrosion damage can be detected. Hence, the AA2024 specimens are losing their ductility potential at higher rates than the AA2198; this proves that Al-Cu-Li alloy seems to be more corrosion resistant than its predecessor, in terms of highly maintaining its ductility characteristics when compared to the Al-Cu alloy for the same exposure time.

For higher exposure times (> 12 hours) ductility seems to decrease almost linearly with increasing exposure time and therefore one could easily correlate exposure time with increasing corrosion-induced transverse crack length; they act as surface notches which, according to fracture mechanics principles, reduce the ductility of the specimens due to the non-uniform stress field that generates plasticity ahead of the crack tips. This linear regime is evident for both alloys; again AA2198 seems to maintain higher fraction of ductility at heavily corroded cases, thus proving once again its superiority for corrosion resistance against AA2024.

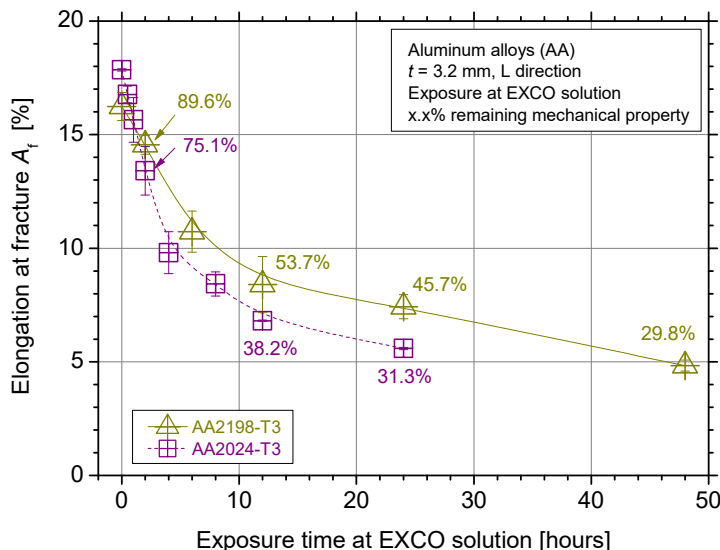


Fig. 5. Elongation at fracture for different exposure time at EXCO solution of aluminum alloys 2024 and 2198.

### 3.2. Fractography

Fig. 6 shows some Scanning Electron Microscopy (SEM) photographs which were taken in order to investigate the fracture mechanism and its correlation along with the corrosion-induced degradation of the specimens. In this direction, three typical specimens were selected. They correspond to 2 h, 6 h and 24 h exposure times and they are shown in Figs. 6a, 6b and 6c, respectively. In full accordance with the surface photographs exhibited in Fig. 2, the surface deterioration of the 2 h exposure specimen is low; it is very interesting however to notice that small pits were also formed at the small surfaces (thickness) of the specimen.

The fracture surface for the case of 2 h and 6 h exposure seems to be unaffected by the corrosion exposure since the classical ductile fracture mechanism is evident with  $45^\circ$  inclination angle, that corresponds to slipping of the shear bands. On the contrary, this classical fracture mechanism is no longer valid for the highly corroded specimen of 24 h exposure (Fig. 6c), where surface deterioration is obvious for both corroded surfaces and the fracture surface seems to be guided by the surface pits on all corroded surfaces. Nevertheless, there is strong evidence that fracture initiated from the region close to the small corroded surfaces. The corrosion resistance of the different surfaces (upper surface or thickness surface) is the subject of a research project in progress and will be reported in a future article of the authors.

### 4. Concluding remarks

The tensile mechanical behavior of two aluminum alloys was experimentally studied. The specimens before tested were pre-corroded in exfoliation corrosion solution for various exposure times. It was definitely concluded that corrosion degrades all aspects of the tensile behavior of the AA2024 alloy at a much higher level compared to the respective degradation of the tensile properties of the AA2198 alloy. This is true for the yield stress, the tensile strength and also the elongation at fracture. It was thus definitely concluded that Al-Cu-Li alloy is superior concerning corrosion resistance, since it maintains higher percentages of the initial (uncorroded) values of its tensile properties, against AA2024.

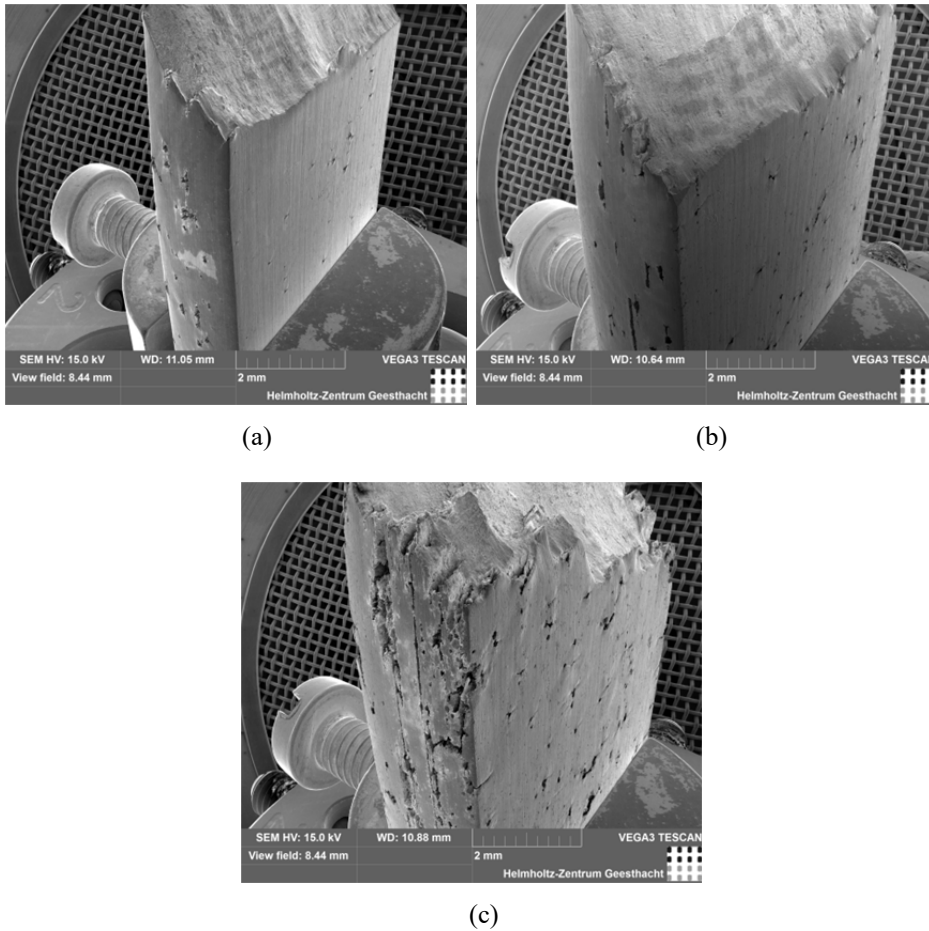


Fig. 6. Fracture surfaces of AA2198 pre-corroded tensile specimens (a) 2 h; (b) 6 h; (c) 24 h.

## References

- Alexopoulos, N.D., Migklis, E., Stylianos, A., Myriounis, D.P., 2013. Fatigue behavior of the aeronautical Al-Li (2198) aluminum alloy under constant amplitude loading”, *International Journal of Fatigue*, 56, 95-105.
- Alexopoulos, N.D., Velonaki, Z., Stergiou, C.I., Kourkoulis, S.K., 2016. The effect of artificial ageing heat treatments on the corrosion-induced hydrogen embrittlement of 2024 (Al–Cu) aluminium alloy. *Corrosion Science*, 102, 413-424.
- Chen, J., Madi, Y., Morgeneyer, T. F., Besson, J., 2011. Plastic flow and ductile rupture of a 2198 Al-Cu-Li aluminum alloy. *Computational Materials Science*, 50, 1365-1371.
- Steglich, D., Wafai, H., Besson, J., 2010a. Interaction between anisotropic plastic deformation and damage evolution in Al 2198 sheet metal. *Engineering Fracture Mechanics*, 77, 3501-3518.
- Steglich, D., Wafai, H., Besson, J., 2010b. Anisotropic deformation and damage in aluminium 2198 T8 sheets. *International Journal of Damage Mechanics*, 19, 131-152.